JOURNAL OF VIROLOGY, Apr. 1992, p. 2076–2085
0022-538X/92/042076-10$02.00/0

Vol. 66, No. 4

An Orthopoxvirus Serpinlike Gene Controls the Ability of Infected Cells To Fuse

PETER C. TURNER AND RICHARD W. MOYER*

Department of Immunology and Medical Microbiology, University of Florida, Gainesville, Florida 32610-0266

Received 19 December 1991/Accepted 13 January 1992

Most orthopoxviruses encode a functional hemagglutinin (HA), which is nonessential for virus growth in cell culture. However, inactivation of the HA gene leads to the formation of polykaryocytes (syncytia) by fusion of infected cells at neutral pH. Fusion is not observed when a functional HA gene is present. Deletion of open reading frames (ORFs) K2, K3, and K4 within the *Hin*dIII K fragment of the HA-positive (HA^+) vaccinia virus strain WR also led to fusion of cells upon infection at neutral pH. A novel ORF inactivation procedure utilizing the polymerase chain reaction was used to specifically implicate the K2 ORF in this phenomenon. The K2 ORF (the viral SPI-3 gene) encodes a protein resembling serine protease inhibitors (serpins). Inactivation of the SPI-3 gene in any of the HA^+ orthopoxviruses tested caused infected cells to fuse in a manner which appeared identical to that seen for HA^- mutants, although fusion was most pronounced with cowpox virus. SPI-3-negative strains fused despite the fact that the HA was expressed and processed normally, i.e., cells infected with SPI-3 mutants remained functionally hemadsorption positive, and analysis of the HA protein by Western immunoblot suggested that posttranslational modifications of the HA protein appeared normal. Fusion triggered by SPI-3 mutants, like that for HA^- mutants, was inhibited by the monoclonal antibody C3 directed against the vaccinia virus 14-kDa envelope protein. Therefore SPI-3- and HA-mediated fusion share a requirement for the 14-kDa protein, suggesting linkage of the seemingly disparate SPI-3 and HA genes through a common pathway which normally acts to prevent fusion of cells infected with wild-type virus.

The orthopoxviruses include the prototype vaccinia virus (VV), the closely related rabbitpox virus (RPV), and cowpox virus (CPV) (19). Studies of poxvirus pathogenesis suggest that many genes involved in virulence and host range are located within the terminal regions of viral DNA which flank a common, internal conserved core of genes (9, 10, 18). Although many of the genes within these terminal regions of DNA are nonessential in tissue culture, they may have important roles in vivo, enabling the virus to evade the host immune response and spread from the initial site of infection. Examples would include the viral genes which encode proteins which resemble plasma serine protease inhibitors (serpins).

Serpinlike genes have been found in CPV (22), VV (5, 17, 28), fowlpox virus (29), and the leporipoxviruses malignant rabbit fibroma virus, and myxoma virus (30). In orthopoxviruses there are three members of this viral gene family, designated SPI-1, SPI-2, and SPI-3. The CPV SPI-2 gene located toward the right terminus of the genome was originally identified by its role in the production of red pocks on the chicken chorioallantoic membrane (22). The DNA sequence of SPI-2 suggested that the encoded 38-kDa protein might act to inhibit a serine protease involved in blood coagulation; however, more recent studies (21) indicate that the SPI-2 gene product interferes with chemotactic signals involved in the inflammatory response.

VV contains a homolog of the CPV SPI-2 gene, a related SPI-1 gene located near the right terminus of the genome with no known function (17), and a more distantly related SPI-3 gene (open reading frame [ORF] K2) located in the *Hin*dIII K fragment toward the left terminus (5, 12). We show here that the wild-type SPI-3 gene of VV, RPV, and CPV is involved in the inhibition of cell fusion on infection.

Cell-cell fusion or "fusion from within" at neutral pH has been observed for poxvirus mutants, such as VV IHD-W, which are unable to express hemagglutinin (HA) at the cell surface (16). Fusion can also be caused by mutants of VV WR obtained by persistent infection of interferon-treated Friend erythroleukemia cells (25). Wild-type HA-positive (HA^+) VV, which does not cause cell fusion at neutral pH, can be induced to do so by acid pH treatment of infected cells (13).

A 14-kDa protein found as a trimer in the envelope of the intracellular form of VV and on the cell surface has been proposed to be required for virus-induced cell fusion (25). Neutralizing monoclonal antibody MAbC3 directed against the 14-kDa protein (24) inhibits cell fusion triggered by a VV mutant, 87-4, derived from persistent infection (25), by HA^- VV IHD-W, or by acid pH treatment of cells infected with wild-type virus (13). In addition, mutants with N-terminal deletions in the 14-kDa protein cannot induce cell fusion (13). We report here that cell fusion can be caused by SPI-3 mutants of CPV, VV, and RPV and that this fusion appears to be identical to that caused by HA^- strains of virus.

MATERIALS AND METHODS

Viruses and cells. VV strain WR and the HA^- wild-type Utrecht strain of RPV were obtained from the American Type Culture Collection. VV IHD-J and IHD-W (16) were from S. Dales via R. C. Condit. RPV HA^+, a spontaneous HA^+ hemadsorbing revertant derived from wild-type RPV (7) was provided by D. C. Bloom. The wild-type Brighton Red (HA^+) strain of CPV was obtained from David Pickup.

The above viruses were propagated on CV-1 monolayers grown in GIBCO minimum essential medium (MEM) sup-

* Corresponding author.

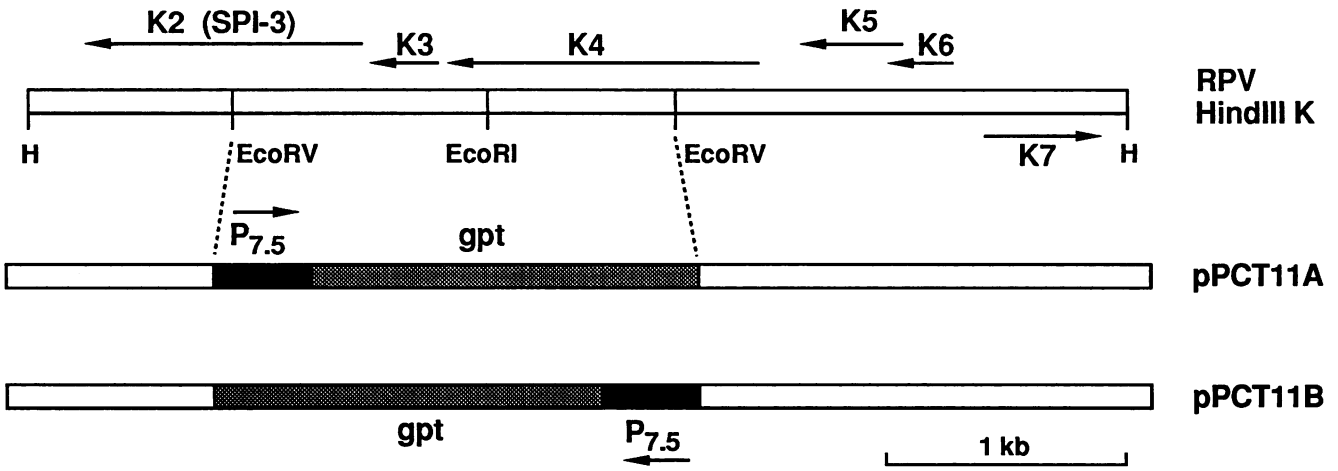

FIG. 1. Positions of ORFs K2, K3, and K4. The top line represents the RPV *Hin*dIII K fragment, showing ORFs K2 to K7 and *Hin*dIII sites (H). Note the *Eco*RI site in ORF K4 into which $P_{7.5}$gpt was inserted in pPCT12. The second and third lines represent pPCT11A and pPCT11B, showing the ΔK234 deletion between the two *Eco*RV sites and replacement of this region with the $P_{7.5}$gpt cassette in both orientations. The vector into which these fragments are cloned, pΔBS, is not shown.

plemented with 7% fetal bovine serum–2 mM glutamine–50 U of penicillin per ml–50 μg of streptomycin per ml–1 mM sodium pyruvate–0.1 mM MEM nonessential amino acids (GIBCO).

Antisera. Monospecific rabbit anti-HA antiserum (27) was provided by S. Dales. Mouse monoclonal antibody MAbC3 against the VV 14-kDa envelope protein (24) was obtained from M. Esteban.

Purification of virus DNA. DNA was isolated by digestion of extracellular virus with 1 mg of proteinase K per ml for 2 h at 50°C in TE (10 mM Tris-HCl [pH 7.5], 1 mM EDTA) containing 1% sodium dodecyl sulfate (SDS). After being extracted with phenol-chloroform, DNA was precipitated and dissolved in TE.

Plasmid constructions. The bacterial *Escherichia coli gpt* gene under control of the VV $P_{7.5}$ promoter (the $P_{7.5}$gpt cassette) was excised as a 2-kb *Eco*RI fragment from pTK61-gpt (11) and cloned into the *Eco*RI site in the polylinker of pBluescript KS(+) (Stratagene) in both orientations to generate pBS-gptA and pBS-gptB. In these plasmids, the $P_{7.5}$gpt cassette is flanked by additional restriction sites, including *Hin*cII and *Sma*I, and by the binding sites for the KS and SK primers (see polymerase chain reaction [PCR] methods below).

The 4.5-kb RPV *Hin*dIII K fragment was supplied by D. C. Bloom as a pUC9 clone. pΔBS, a derivative of pBluescript KS(+), was constructed by deleting 18 bp of the polylinker between the *Eco*RV and *Sma*I sites. This construct lacked *Eco*RV and *Eco*RI restriction sites but still produced a functional β-galactosidase fragment to allow blue-white screening for inserts on indicator medium. The RPV *Hin*dIII K fragment was cloned into the *Hin*dIII site of pΔBS to create pΔBS-K. pPCT11A and pPCT11B, containing the $P_{7.5}$gpt cassette in either of two orientations, were made by removing a 1.8-kb *Eco*RV fragment containing ORF K3 and parts of ORFs K2 and K4 (Fig. 1) from the *Hin*dIII K fragment in pΔBS-K and replacing it with a blunt-ended $P_{7.5}$gpt cassette produced by excision from pBS-gptA as a 2.1-kb *Hin*cII-*Sma*I fragment.

pPCT12 was constructed by inserting the 2-kb *Eco*RI $P_{7.5}$gpt fragment from pTK61-gpt into the unique *Eco*RI site of pΔBS-K, which is located in ORF K4 (Fig. 1).

pHGN4.1 is a derivative of pHGN3.1 (4) and contains a nonfunctional derivative of the VV IHD-J HA gene in which $P_{7.5}$gpt is cloned via a polylinker into the *Nru*I site in the HA gene.

PCR. The $P_{7.5}$gpt cassette was amplified from 1 μg of pBS-gptA DNA by using primers KS (5′-CGAGGTCGACG GTATCG-3′) and SK (5′-TCTAGAACTAGTGGATC-3′), which flank the *Eco*RI site in pBluescript. RM137 (5′-CCCGGGATCCTGCAGGCCTGAATTCATGATTGCGT TATTG-3′) and RM139 (5′-CGATACCGTCGACCTCGGT TGATAATACGACGGT-3′) were used to amplify the left arm of the SPI-3 gene (SPI-3_L) from 1 μg of CPV genomic DNA. Regions matching the sequence of the RPV SPI-3 gene are underlined. The first 17 bases of RM139 were complementary to primer KS. The right arm of the CPV SPI-3 gene (SPI-3_R) was amplified with primers RM140 (5′-GATCCACTAGTTCTAGATGGTCGTTTCAATTAGG-3′) and RM 138 (5′-CCCGGGCAGCTGAAGCTTCCTTA CACCGTACCCA-3′); the 5′ end of RM140 was complementary to primer SK. The locations of these primers are shown in Fig. 2.

The $P_{7.5}$gpt, SPI-3_L, and SPI-3_R PCR products were

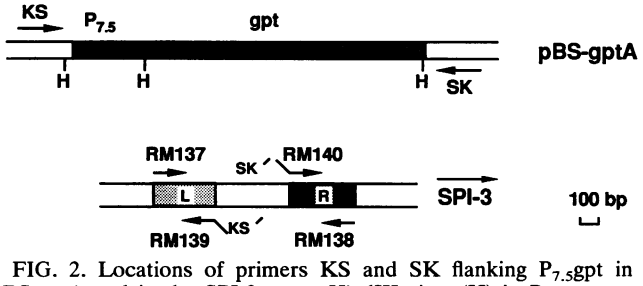

FIG. 2. Locations of primers KS and SK flanking $P_{7.5}$gpt in pBS-gptA and in the SPI-3 gene. *Hin*dIII sites (H) in $P_{7.5}$gpt are shown. The straight arrow above SPI-3 represents the direction of transcription. The orientation of SPI-3 here is opposite to that in the RPV and VV genome maps, in which transcription is from right to left. SPI-3_L and SPI-3_R, the left and right arms of the SPI-3 gene, are indicated by L and R, respectively. Note that the tail of primer RM139 consists of KS′, the complement of primer KS. Similarly, the 5′ region of primer RM140 is complementary to primer SK.

purified on Sephacryl S-400 spun columns (Pharmacia) according to the manufacturer's instructions. SPI-3_L and $P_{7.5}$gpt were joined by mixing the two purified DNAs (each one-tenth of the product from a 100-μl reaction) and amplifying them with the outside primers RM137 and SK. The first two cycles were denaturation at 94°C for 1 min, slow cooling (ramp rate of 10 s per degree C) of to 35°C for 2 min, and extension at 72°C for 3 min (ramp rate of 2 s per degree C). The next 12 cycles were 94°C for 1 min, 50°C for 1 min, and 72°C for 3 min. Extensions were completed by a final incubation at 72°C for 7 min.

$P_{7.5}$gpt and SPI-3_R were joined by the same procedure, using the appropriate outside primers. SPI-3_L-$P_{7.5}$gpt-SPI-3_R was assembled by mixing purified SPI-3_L-$P_{7.5}$gpt and $P_{7.5}$gpt-SPI-3_R (each 1/100 of PCR product from the previous reactions) and using the PCR conditions described above, except that the second set of cycles consisted of 14 repetitions. Product DNA was extracted with phenol-chloroform (1:1) before being transfected into infected cells.

Construction of recombinant viruses. Plasmid or PCR product DNA was transfected by using Lipofectin reagent (GIBCO-Bethesda Research Laboratories) into cells infected with VV, RPV, or CPV. Recombinant viruses containing the *E. coli* xanthine-guanine phosphoribosyltransferase (*gpt*) gene were selected by resistance to mycophenolic acid (MPA) (6, 11). *gpt* selection medium contained 2.5 μg of MPA per ml, 250 μg of xanthine per ml, and 15 μg of hypoxanthine per ml.

CV-1 cells grown to 80% confluence on 60-mm-diameter dishes were infected at a multiplicity of 0.05. Thirty micrograms of Lipofectin (1 mg/ml) was diluted to 50 μl with H_2O in a polystyrene tube. Five micrograms of plasmid DNA or 1 μg of PCR product DNA, in a total volume of 50 μl, was added to the diluted Lipofectin and incubated at room temperature for 15 min to allow complex formation. After adsorption for 2 h at 37°C, the virus inoculum was removed and the dishes were washed twice with serum-free medium. Fresh serum-free *gpt* selection medium (3 ml per dish) was added, followed by the addition of 100 μl of Lipofectin-DNA complex. After 24 h at 37°C, 3 ml of *gpt* selection medium with 7% fetal bovine serum was added. The cells were harvested at 48 h postinfection.

Confluent monolayers of CV-1 cells were pretreated for 14 to 24 h with *gpt* selection medium before infection with virus resulting from the transfections. MPA-resistant (MPA^r) plaques were visualized after 3 days by staining with neutral red (GIBCO-Bethesda Research Laboratories). Recombinants were plaque purified at least twice before amplification to produce virus stocks.

Hemadsorption assay. Viruses were plaqued on CV-1 monolayers under liquid for 24 to 32 h. Infected monolayers were washed with phosphate-buffered saline (PBS; 0.01 M sodium phosphate, 0.15 M NaCl, pH 7.2), and to each 60-mm dish 2 ml of a 0.5% suspension (packed cells per total volume) of chicken erythrocytes was added. The chicken erythrocytes were washed twice with PBS before use. After being incubated at 37°C for 15 min with occasional agitation, unadsorbed erythrocytes were removed and the monolayers were washed with PBS at 37°C to reduce background adsorption. Plaques were scored as hemadsorption positive (HAD^+) or hemadsorption negative (HAD^-) both microscopically and by the naked eye.

HA activity was quantitated by an end point hemagglutination assay (16). CV-1 monolayers in 60-mm-diameter dishes were infected at a multiplicity of 1. After 24 h, the infected cells were harvested and sonicated in 1 ml of PBS. Fifty microliters of twofold serial dilutions (in PBS) was added to 50 μl of a 0.5% suspension of chicken erythrocytes. Hemagglutination was scored after incubation for 1 h at 37°C in a 96-well conical bottom microtiter plate.

Western immunoblot analysis. Direct analysis of the HA protein was by an immunoblot method similar to that previously described (8). Confluent 150-mm-diameter dishes of CV-1 cells (4×10^7 cells per dish) were infected at a multiplicity of 5. Cells from each dish were harvested at 20 h postinfection and resuspended in 0.5 ml of PBS containing 5 mM phenylmethylsulfonyl fluoride and 10 Kallikrein units of aprotinin per ml. The infected cell suspension was sonicated before the addition of 2× sample buffer (160 mM Tris-HCl [pH 8.9], 4% SDS, 4% 2-mercaptoethanol, 10% glycerol, 5 M

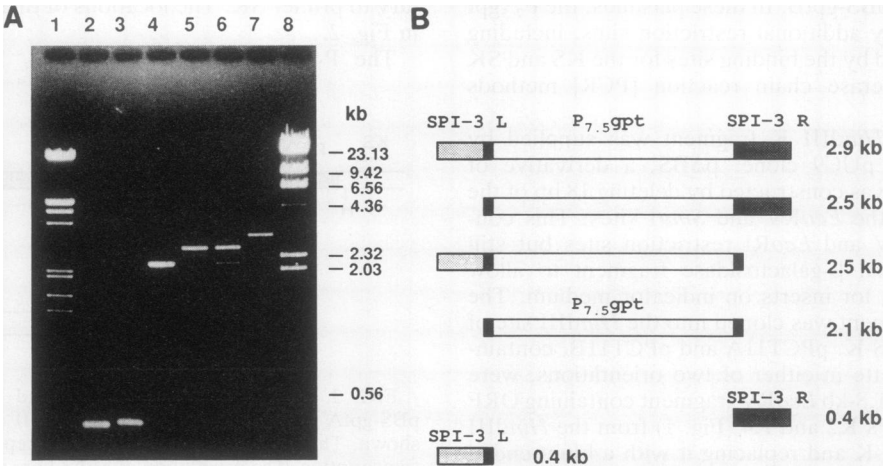

FIG. 3. (A) Ethidium bromide-stained gel showing the PCR products corresponding to the $P_{7.5}$gpt cassette, the left and right individual arms of the CPV SPI-3 gene, and the assembly products generated by recombinant PCR, such that $P_{7.5}$gpt is flanked by SPI-3_L and SPI-3_R. Lanes: 1, λ *Hin*dIII *Eco*RI DNA marker; 2, SPI-3_L; 3, SPI-3_R; 4, $P_{7.5}$gpt; 5, SPI-3_L-$P_{7.5}$gpt; 6, $P_{7.5}$gpt-SPI-3_R; 7, SPI-3_L-$P_{7.5}$gpt-SPI-3_R; 8, λ *Hin*dIII DNA marker. The sizes of λ *Hin*dIII fragments are shown. (B) Structures of the various PCR products shown in panel A. Overlapping regions at the ends are represented by black boxes. Sizes are indicated on the right.

urea, 0.02 M disodium EDTA, and 0.012% bromphenol blue). Samples were sheared by passage through a 26-gauge needle, boiled for 2 min, and loaded onto a 20-cm 7.5% SDS-polyacrylamide gel (50 μg of protein per well). Electrophoresis was in Tris-glycine buffer (25 mM Tris-HCl, 192 mM glycine, 0.1% SDS). Proteins were transferred to 0.1-μm-pore-size nitrocellulose by electrophoresis in transfer buffer (25 mM Tris-HCl, 192 mM glycine, 20% methanol) at 250 mA for 3 h at 4°C. The blot was blocked with BLOTTO (10 mM Tris-HCl [pH 8.0], 150 mM NaCl, 0.5% dry milk) for 2 h at room temperature before the addition of a 1:2,000 dilution of rabbit anti-HA antiserum in BLOTTO. Incubation was for 18 h at room temperature. The blot was washed three times in TBS (10 mM Tris-HCl [pH 8.0], 150 mM NaCl) for 15 min per wash. A 1:1,000 dilution in BLOTTO of alkaline phosphatase-conjugated goat anti-rabbit immunoglobulin (Fisher Biotech) was added, and the blot was incubated for 90 min at room temperature before being washed three times in TBS for 15 min. Developing solution (100 mM Tris-HCl [pH 9.5], 100 mM NaCl, 5 mM $MgCl_2$) containing 330 μg of nitroblue tetrazolium per ml and 165 μg of 5-bromo-4-chloro-3-indolyl phosphate per ml was added. After 15 min, TE was added to stop development.

RESULTS

Inactivation of ORFs K2, K3, and K4. In order to assess the effects on the virus of inactivating ORFs in the *Hin*dIII K fragment of VV and RPV, plasmids pPCT11A and pPCT11B were made as described in Materials and Methods. This work was part of an ongoing investigation of the role of serpinlike genes in pock color on the chorioallantoic membrane and in pathogenicity. These constructs carry a derivative of the RPV *Hin*dIII K fragment which bears a 1.8-kb deletion, ΔK234, between two *Eco*RV sites. The deleted region, consisting of the entire K3 ORF and parts of ORFs K2 and K4, has been replaced with the $P_{7.5}$gpt cassette in both possible orientations (Fig. 1). After infection of CV-1 cells with wild-type VV WR, pPCT11A or pPCT11B DNA (Fig. 1) was introduced by transfection. MPA^r virus resulting from homologous recombination was selected and further plaque purified twice under selective conditions before amplification.

During growth on CV-1 cells of VV WR recombinants generated from transfections with pPCT11A or pPCT11B, it became obvious that instead of the usual cytopathic effect, cell fusion was occurring at neutral pH to produce giant cells. Identical results were observed for recombinant viruses containing $P_{7.5}$gpt in either orientation. Similar derivatives of the HA^+ VV IHD-J strain were constructed, using pPCT11A or pPCT11B plasmid DNA, and again the resulting recombinants bearing deletions of the *Hin*dIII K fragment between the two *Eco*RV sites (ΔK234 virus) caused fusion on infection of CV-1 cells. The syncytial phenotype observed was very similar to that of the HA^- VV IHD-W strain (16; see Fig. 8E). Both HA^- VV IHD-W and wild-type RPV, which is naturally HA^-, cause cell fusion. Engineering of the ΔK234 deletion (Fig. 1) into either of these two viruses had no effect on the syncytium-forming property of the virus. Spontaneous HA^+ revertants of HA^- wild-type RPV (7) no longer cause cell fusion; however, RPV HA^+ ΔK234 recombinants produced giant cells and fusion which were apparently identical to those generated by wild-type RPV (HA^-).

On the assumption that the arrangement and sequence of ORFs K2, K3, and K4 were conserved in CPV, we transfected CPV-infected CV-1 cells with pPCT11A and pPCT11B DNA. MPA^r CPV recombinants fused CV-1 cells on infection to produce giant cells that were larger than those seen for ΔK234 derivatives of VV or HA^+ RPV. Plaques of the CPV recombinants containing the $P_{7.5}$gpt cassette were also much larger than those of wild-type CPV and could be readily distinguished by the naked eye because they contained polykaryocytes which were intensely stained by neutral red. CPV was chosen for further study since the fusion phenomenon was most dramatic in this orthopoxvirus.

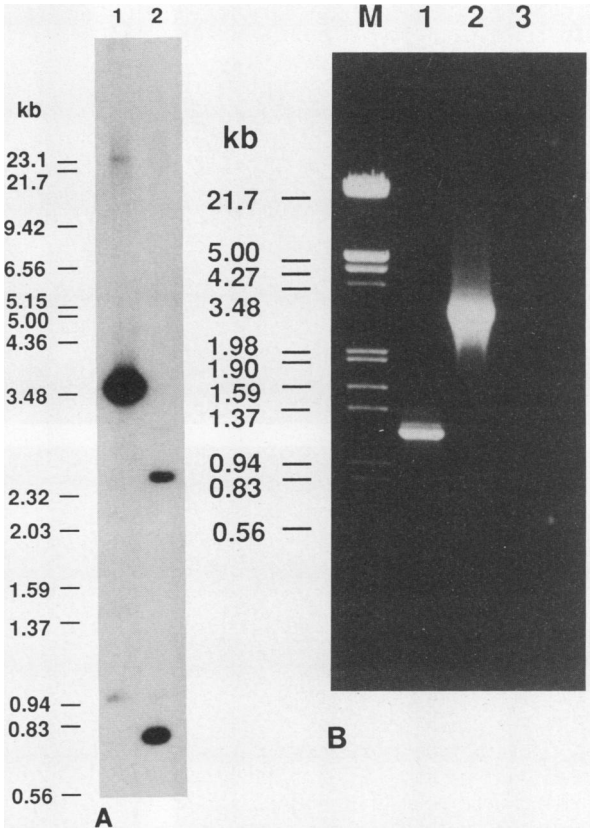

FIG. 4. Verification of CPV ΔK2. (A) Southern blot of genomic DNA restricted with *Hin*dIII. The probe was specific for the SPI-3 gene. Lanes: 1, wild-type CPV; 2, CPV ΔK2. The sizes of DNA standards are indicated on the left. (B) Ethidium bromide-stained gel of PCR products generated from CPV DNA with primers RM137 and RM138. Lanes: M, marker (λ DNA digested with *Hin*dIII and *Eco*RI); 1, wild-type CPV; 2, CPV ΔK2; 3, control (no template DNA). The sizes of DNA standards are shown on the left.

Three ORFs are presumably inactivated by the ΔK234 deletion in pPCT11A and pPCT11B. ORF K3, which is completely deleted in the above plasmids, has recently been shown to encode a eukaryotic initiation factor 2 alpha homolog and is responsible for interferon resistance (2). No connection between ORF K3 and cell fusion has been reported. ORF K4 (5, 12) is related to the gene encoding the major 37-kDa envelope antigen (15). ORF K2 (5, 12), which we have designated SPI-3, is a serine protease inhibitor-like gene with no reported function. The pPCT12 construct (see Materials and Methods) carries the RPV *Hin*dIII K fragment with $P_{7.5}$gpt inserted at the *Eco*RI site within ORF K4 (Fig. 1). pPCT12 DNA was transfected into CV-1 cells infected with wild-type CPV, and MPA^r recombinants were isolated, purified, and amplified. None of the recombinants produced syncytial plaques or cell fusion at a high multiplicity of

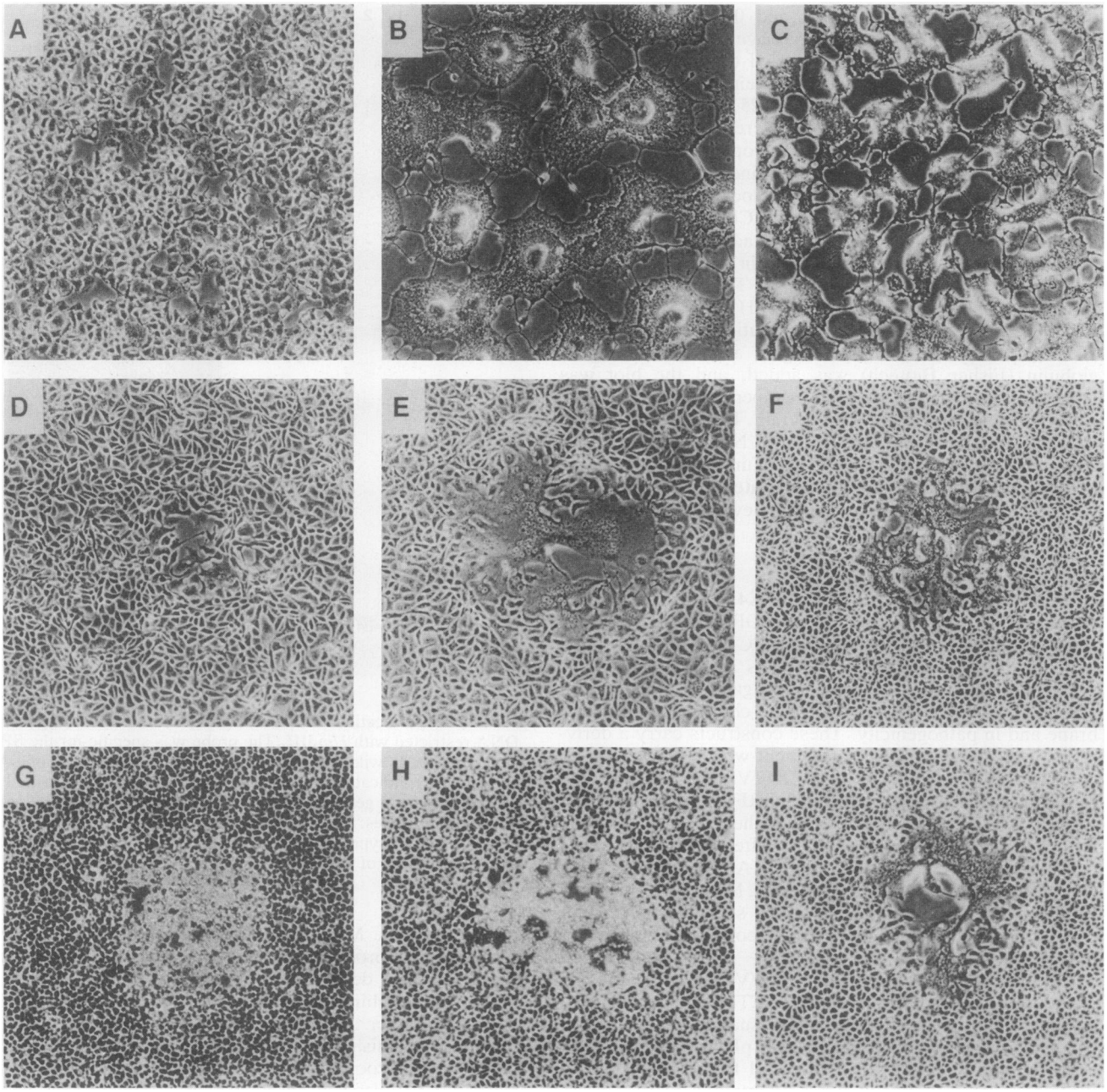

FIG. 5. CPE, plaques, and hemadsorption assay for CPV derivatives on CV-1 monolayers. Infected cells were incubated for 24 h in liquid medium. The top row shows CPE produced by wild-type CPV at a multiplicity of infection of 10 (panel A), CPV ΔK2 at a multiplicity of 1 (panel B), and CPV HA::gpt at a multiplicity of 1 (panel C). The middle row shows the plaque morphology of wild-type CPV (panel D), CPV ΔK2 (panel E), and CPV HA::gpt (panel F). The bottom row shows the results of testing plaques of wild-type CPV (panel G), CPV ΔK2 (panel H), and CPV HA::gpt (panel I) for the ability to adsorb chicken erythrocytes. The bound erythrocytes appear as bright objects under phase contrast.

infection. This result suggests that the ORF K4 homolog in CPV is not involved in the cell fusion phenomenon and is consistent with the observation that inactivation of ORF K4 in VV IHD-J had no obvious effects on infection (3).

Inactivation of ORF K2 (SPI-3). A novel PCR-based scheme, described in more detail elsewhere (29a), was used to create a deletion in the ORF K2 (SPI-3) homolog of CPV. The object was to determine whether inactivation of SPI-3 was responsible for the cell fusion observed with CPV ΔK234. The $P_{7.5}$gpt cassette from pBS-gptA was amplified by using the flanking 17-base primers KS and SK (Fig. 2 and Fig. 3A, lane 4). Primers to amplify the left and right arms of the SPI-3 gene (Fig. 2) were designed on the basis of the RPV SPI-3 sequence (3a). Primer pairs RM137 + RM139 and RM140 + RM138 each gave a PCR product of the expected size (391 and 404 bp, respectively) from RPV DNA (data not shown), and the corresponding CPV PCR products were apparently of identical size (Fig. 3A, lanes 2 and 3).

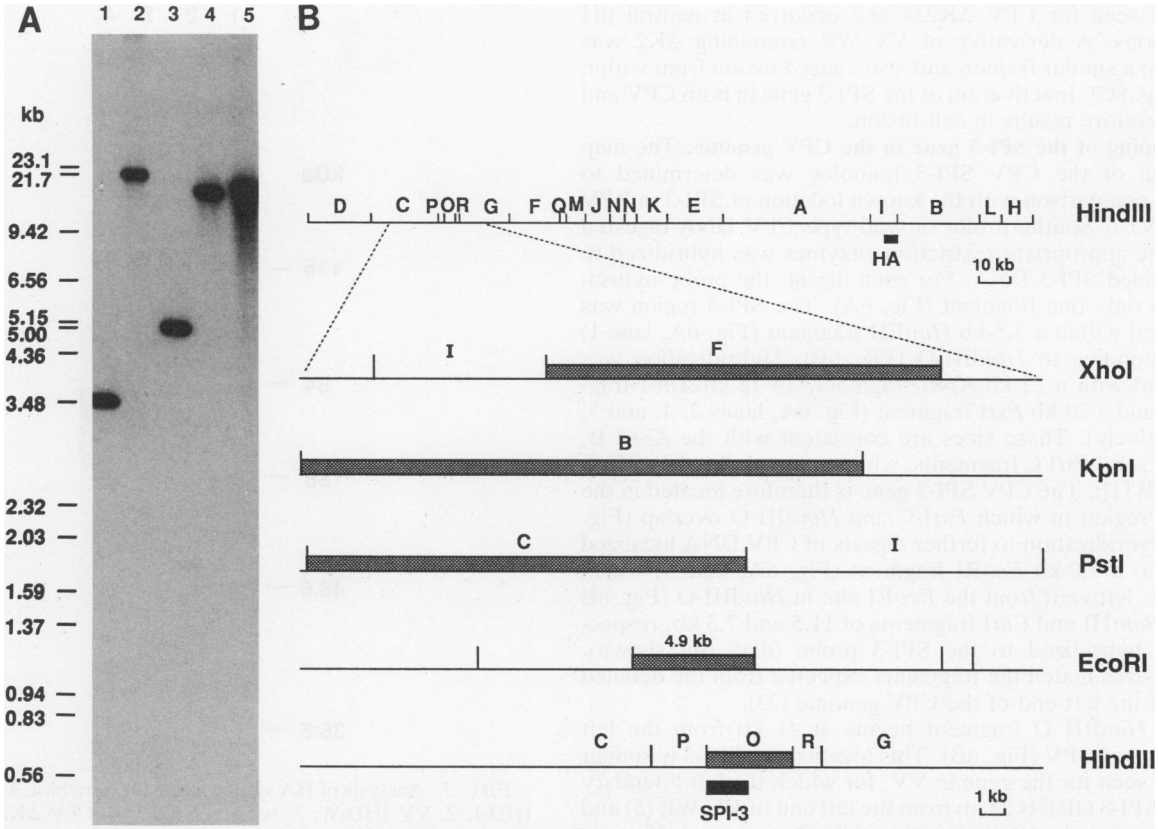

FIG. 6. Mapping of the CPV SPI-3 gene. (A) Southern blot of CPV DNA digested with *Hin*dIII (lane 1), *Kpn*I (lane 2), *Eco*RI (lane 3), *Xho*I (lane 4), and *Pst*I (lane 5). The probe was ^{32}P-labeled SPI-3 PCR product from amplification of RPV DNA with RM137 and RM138. Sizes of DNA standards are indicated on the left. (B) The top line represents the *Hin*dIII map of CPV. The lines below represent an enlargement of the region indicated by the dotted lines. Vertical lines represent restriction sites for the enzyme shown on the right. Shaded boxes indicate restriction fragments that hybridized to the SPI-3 probe (panel A). The SPI-3 gene is located in the black box at the bottom, which is defined by the overlap between the *Pst*I C and *Hin*dIII O fragments. The position of the HA gene in the *Hin*dIII I fragment is also indicated.

The $P_{7.5}$gpt PCR product was flanked with the left and right arms of the CPV SPI-3 gene (SPI-3_L and SPI-3_R) by means of recombinant PCR (14). Primers RM139 and RM140 were designed so that each had a 5′ tail complementary to one of the primers flanking $P_{7.5}$gpt in pBS-gptA (Fig. 2). SPI-3_L and $P_{7.5}$gpt (Fig. 2 and 3) were mixed, denatured, and annealed to allow strands from the two PCR products to form heteroduplexes by means of the 17-base overlap. Heteroduplexes with recessed 3′ ends were extended by *Taq* DNA polymerase to produce a joint SPI-3_L-$P_{7.5}$gpt double-stranded DNA, which was amplified by using the outside primers RM137 and SK (Fig. 3, lane 5). $P_{7.5}$gpt was joined to SPI-3_R by a similar strategy and amplified with primers KS and RM138 (Fig. 3, lane 6). The SPI-3_L-$P_{7.5}$gpt and $P_{7.5}$gpt-SPI-3_R intermediates were mixed, denatured, annealed, extended, and amplified with primers RM137 and RM138 to generate the final 2.9-kb construct SPI-3_L-$P_{7.5}$gpt-SPI-3_R (Fig. 3, lane 7). This linear DNA was transfected directly into CV-1 cells infected with wild-type CPV, and MPA^r virus was selected.

The effect of homologous recombination between SPI-3_L-$P_{7.5}$gpt-SPI-3_R and the wild-type SPI-3 gene of CPV is to delete the region of SPI-3 between SPI-3_L and SPI-3_R (Fig. 2) and replace it with the $P_{7.5}$gpt cassette. The presence of the K2 deletion in the MPA^r recombinants was confirmed by Southern blot analysis and by PCR. A SPI-3-specific probe was made by amplifying the RPV SPI-3 gene with RM137 and RM138 and ^{32}P-labeling the resulting 1.2-kb PCR product. The probe hybridized to a 3.5-kb *Hin*dIII fragment from wild-type CPV DNA and to *Hin*dIII fragments of 2.4 and 0.8 kb from CPV ΔK2 DNA (Fig. 4A, lanes 1 and 2, respectively), confirming that the $P_{7.5}$gpt insertion was within the SPI-3 gene. The sizes of the two novel *Hin*dIII fragments were consistent with the size of the SPI-3 deletion (410 bp on the basis of the RPV SPI-3 sequence) and the locations of *Hin*dIII restriction sites within the $P_{7.5}$gpt PCR product (Fig. 2) which had been inserted.

PCR amplification of wild-type CPV DNA with primers RM137 and RM138 gave a 1.2-kb product, which was replaced with a 3-kb product in CPV ΔK2 (Fig. 4B, lanes 1 and 2, respectively). This finding was consistent with the deletion of 0.4 kb from the SPI-3 gene and the insertion of the 2.1-kb $P_{7.5}$gpt cassette and showed that the CPV ΔK2 virus stock was not contaminated with wild-type CPV. The orientation of $P_{7.5}$gpt in CPV ΔK2 was confirmed by using a primer specific for $P_{7.5}$ with either RM137 or RM138 in PCR (data not shown).

After 24 h, wild-type CPV produced minimal cytopathic effect (CPE) on infection of CV-1 cells at high multiplicity (Fig. 5A), but CPV ΔK2 produced giant cells under similar conditions (Fig. 5B). In contrast with the small plaques of wild-type CPV, which did not show extensive fusion of infected cells (Fig. 5D), CPV ΔK2 gave large syncytial plaques (Fig. 5E). The phenotype for CPV ΔK2 was identical

to that seen for CPV ΔK234 and occurred at neutral pH conditions. A derivative of VV WR containing ΔK2 was made in a similar fashion and also caused fusion from within (see Fig. 8C). Inactivation of the SPI-3 gene in both CPV and VV therefore results in cell fusion.

Mapping of the SPI-3 gene in the CPV genome. The map position of the CPV SPI-3 homolog was determined to enable comparison with the known location of SPI-3 in RPV and VV. A Southern blot of wild-type CPV DNA digested with the appropriate restriction enzymes was hybridized to ^{32}P-labeled SPI-3 DNA. For each digest, the probe hybridized to only one fragment (Fig. 6A). The SPI-3 region was localized within a 3.5-kb *Hin*dIII fragment (Fig. 6A, lane 1) corresponding to *Hin*dIII-O (Fig. 6B). Hybridization was detected with a 22-kb *Kpn*I fragment, an 18-kb *Xho*I fragment, and a 20-kb *Pst*I fragment (Fig. 6A, lanes 2, 4, and 5, respectively). These sizes are consistent with the *Kpn*I B, *Xho*I F, and *Pst*I C fragments, which each overlap *Hin*dIII-O (Fig. 6B [1]). The CPV SPI-3 gene is therefore located in the 1.7-kb region in which *Pst*I-C and *Hin*dIII-O overlap (Fig. 6B). Hybridization to further digests of CPV DNA localized SPI-3 to a 5.0-kb *Eco*RI fragment (Fig. 6A, lane 3) which extends leftward from the *Eco*RI site in *Hin*dIII-O (Fig. 6B [23]). *Bam*HI and *Cla*I fragments of 11.5 and 7.3 kb, respectively, hybridized to the SPI-3 probe (data not shown). These sizes match the fragments expected from the detailed map of the left end of the CPV genome (23).

The *Hin*dIII O fragment begins at 41 kb from the left terminus of CPV (Fig. 6B). This location for SPI-3 is similar to that seen for the gene in VV, for which the left boundary of the SPI-3 ORF is 24 kb from the left end of VV WR (5) and 29.2 kb from the left terminus of VV Copenhagen (12).

Construction of CPV HA::gpt and mapping of the CPV HA gene. The ability of poxviruses to cause cell fusion generally correlates strongly with a lack of HA production (16). An HA-negative derivative of wild-type CPV was made to allow comparison with CPV ΔK2. CPV HA::gpt was constructed by transfecting CPV-infected CV-1 cells with pHGN4.1 DNA, which contains a copy of the VV IHD-J HA gene which has been inactivated by insertion of $P_{7.5}$gpt (see Materials and Methods) and selection for MPA^r virus recombinants. The cell fusion properties of CPV HA::gpt were indistinguishable from those of CPV ΔK2 (Fig. 5). CPV HA::gpt produced giant cells and syncytial plaques on infection of CV-1 cells (Fig. 5C and F, respectively). Fusion from within can therefore be triggered by mutation of either the HA or SPI-3 gene of CPV.

The HA gene of CPV was also mapped by Southern blot hybridization, using a probe derived from PCR amplification of the VV WR HA gene. In CPV, the HA gene is located in a 4.2-kb region in the 9.6-kb *Hin*dIII I fragment (Fig. 6B) which is defined by overlap with the 11-kb *Pst*I J fragment. The HA probe also hybridized with the 20-kb *Kpn*I C fragment and with *Bam*HI, *Eco*RI, and *Cla*I fragments of 11, 10, and 2.5 kb, respectively (data not shown). These data are consistent with the HA location shown in Fig. 6B and the detailed map of the right-hand end of the CPV genome (23). The position of the HA gene in CPV is similar to its location in VV (12).

HA production by SPI-3 mutants of CPV, RPV, and VV. Does mutation in SPI-3 cause cell fusion by interfering with the synthesis, posttranslational modification, or membrane localization of HA? This question was first addressed by testing cells infected with SPI-3 mutants for the ability to hemadsorb (see Materials and Methods). The results (Table 1, Fig. 5) indicate that all SPI-3 mutants containing a wild-type HA gene qualitatively retain the ability to adsorb chicken erythrocytes. This is true for all CPV, RPV, and VV strains tested. The adsorption of chicken erythrocytes to the syncytial plaques of CPV ΔK2 (Fig. 5H) represents a novel phenotype and demonstrates that mutation in a gene other than HA can cause fusion from within. Syncytial plaques of CPV HA::gpt were HAD$^-$ by this test (Fig. 5I), as expected, and wild-type CPV plaques were HAD$^+$ (Fig. 5G). No quantitative difference in measurable HA activity could be detected between wild-type CPV and CPV ΔK2. The HA titer (reciprocal of the highest dilution of infected cell lysate that has hemagglutination activity) was 2,048 for both viruses.

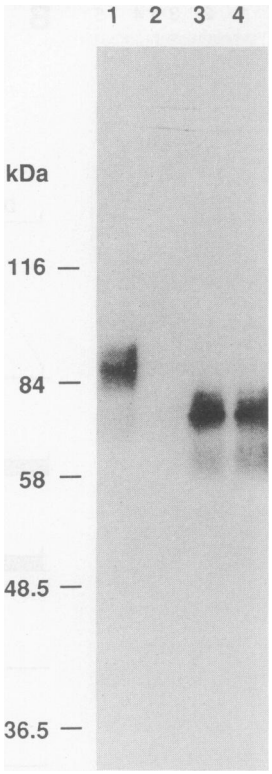

FIG. 7. Analysis of HA synthesis by Western blot. Lanes: 1, VV IHD-J; 2, VV IHD-W; 3, wild-type CPV; 4, CPV ΔK234. Marker sizes are indicated on the left.

The presence and state of the HA protein in total extracts of infected cells was investigated by Western blotting, using monospecific rabbit anti-HA antiserum. The VV HA ORF encodes a polypeptide of 35 kDa. Posttranslational modifications of the polypeptide lead to an apparent electrophoretic mobility of 85 kDa for the fully modified protein. HA protein of about 85 kDa was readily detectable in VV IHD-J extract but not in the VV HA$^-$ IHD-W strain (Fig. 7, lanes 1 and 2, respectively), confirming the specificity of the antibody. The quantity of HA protein and its migration rate on an SDS–7.5% polyacrylamide gel appeared to be identical for both wild-type CPV and CPV ΔK234 (Fig. 7, lanes 3 and 4), although the CPV HA protein appeared to be smaller than that for VV. No differences in HA production or processing between wild-type CPV and CPV ΔK234 could be detected by using the method described here. It is possible, but unlikely, that in SPI-3 mutants the HA protein is altered such that hemadsorption activity is retained but inhibition of cell

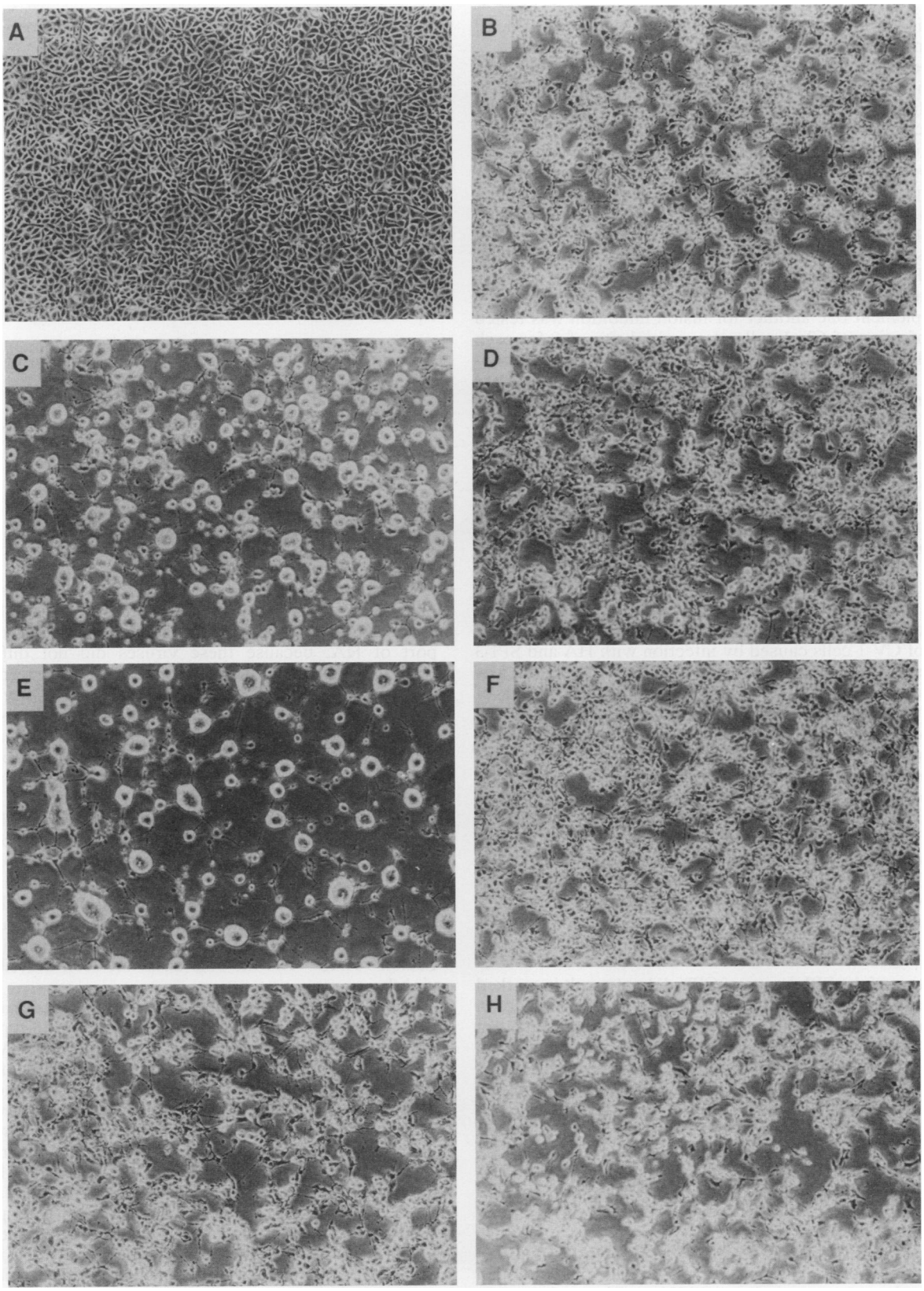

FIG. 8. Effect of MAbC3 and mixed infection on cell fusion. Confluent CV-1 monolayers were infected with the indicated viruses, each at a multiplicity of 5. The virus inoculum was removed after adsorption for 1.5 h, and the monolayers were washed with PBS. Medium containing 2% fetal bovine serum with or without MAbC3 (1:100 dilution) was added, and infected cells were photographed at 24 h postinfection, using a phase-contrast microscope. Panels: A, uninfected cells; B, VV WR; C, VV WR ΔK2; D, VV WR ΔK2 plus MAbC3; E, VV IHD-W; F, VV IHD-W plus MAbC3; G, coinfection with VV WR ΔK2 and IHD-W; H, VV IHD-J.

fusion is lost. More sensitive techniques may be capable of detecting a subtle modification of this type.

Mixed infections. Coinfection at high multiplicity of HeLa cells with VV IHD-J (HA^+) and IHD-W (HA^-) did not lead to cell fusion (16), indicating that IHD-J was able to suppress fusion caused by IHD-W by supplying wild-type HA protein. Mixed infection of CV-1 cells with wild-type CPV and CPV ΔK2, both at a multiplicity of 5, gave CPE characteristic of wild-type CPV alone, i.e., fusion was not observed (data not shown). This result suggested that the defect in SPI-3 protein production by CPV ΔK2 could likewise be overcome by expression of functional SPI-3 gene product from the wild-type CPV genome.

The ability of CPV ΔK2 (ΔSPI-3) and CPV HA::gpt (HA^-) to complement one another for fusion inhibition was tested by coinfection of CV-1 cells at a multiplicity of 5 for each virus. Fusion was greatly reduced (data not shown), confirming that the lesions in the two viruses, as expected, were in different genes. The same result was seen in an analogous mixed infection with VV WR ΔK2 and VV IHD-W, which produced wild-type CPE (Fig. 8G). These genetic experiments support the idea that a cell fusion pathway can be unmasked by mutation in either the HA or SPI-3 gene and that mutations in either gene can be complemented in *trans*.

Effect of a monoclonal antibody against the 14-kDa virus envelope protein. MAbC3, a monoclonal antibody against the 14-kDa virus envelope protein, has been shown to block fusion from within (25). The cell fusion pathway appears to be sensitive to inhibition by MAbC3 regardless of how fusion is triggered (13). We tested MAbC3 for the ability to inhibit fusion of CV-1 cells caused by infection with HA and SPI-3 mutants. Fusion triggered by VV IHD-W infection was abolished by MAbC3 (Fig. 8F), confirming the results of Gong et al. (13). Treatment with MAbC3 converted the CPE produced by VV IHD-W into the type normally seen on infection with VV IHD-J alone (Fig. 8H).

MAbC3 reduced fusion induced by infection with CPV ΔK2, but inhibition was not complete at a 1:50 dilution of MAbC3 (data not shown). However, a 1:100 dilution of MAbC3 gave complete inhibition of fusion by VV WR ΔK2, such that the CPE was indistinguishable from that of wild-type VV WR (Fig. 8D and B, respectively). Fusion induced by SPI-3 mutants therefore involves the 14-kDa protein.

TABLE 1. Cell fusion and hemadsorption properties of VV, RPV, and CPV derivatives

Virus	Cell fusion[a]	Hemadsorption
VV WR	−	+
VV WR ΔK234[b]	+	+
VV WR ΔK2[c]	+	+
VV IHD-J	−	+
VV IHD-J ΔK234	+	+
VV IHD-W	+	−
VV IHD-W ΔK234	+	−
RPV	+	−
RPV ΔK234	+	−
RPV HA^+	−	+
RPV HA^+ ΔK234	+	+
CPV	−	+
CPV ΔK234	++	+
CPV ΔK2	++	+
CPV HA::gpt	++	−

[a] −, no fusion; +, small polykaryocytes; ++, large polykarocytes.
[b] ΔK234 strains contain mutations in ORFs K2, K3, and K4.
[c] ΔK2 strains contain a mutation in ORF K2.

DISCUSSION

Deletion of the SPI-3 gene of CPV did not result in marked changes in pock color on the chorioallantoic membrane or in virulence to mice after intranasal inoculation (data not shown); however, this gene clearly acts in wild-type virus to inhibit cell-cell fusion at neutral pH. Mutation of the SPI-1 gene of CPV had no effect on CPE in vitro (data not shown), and CPV SPI-2 mutants have not been reported to cause cell fusion. The nucleotide sequences of the VV WR serpin genes are consistent with a distinct function for the SPI-3 gene compared with those of SPI-1 and SPI-2. The SPI-3 protein is only 25 and 23% identical with those of SPI-1 and SPI-2, respectively, but SPI-1 and SPI-2 share 47% amino acid identity.

The position of the SPI-3 gene in CPV (Fig. 6B) is very similar to its location in VV (5, 12) and in RPV (3a), although the direction of transcription in CPV remains to be established. The function of SPI-3 appears to be similar in the closely related orthopoxviruses VV, RPV, and CPV. The fact that CPV ΔK2 was more fusogenic than VV WR ΔK2 is under investigation and presumably reflects a more efficient or abundant fusion apparatus or possibly a reduced cytocidal effect compared with that of VV.

Although the fusion properties of SPI-3 mutants resembled those of HA mutants, mutation in the SPI-3 gene apparently did not affect the synthesis or membrane transport of HA, because these viruses did not differ from wild-type in hemadsorption (Table 1) or in a Western blot for HA protein (Fig. 7). The HA protein of wild-type CPV migrated on SDS-polyacrylamide gel electrophoresis with an apparent size of about 72 kDa, compared with 85 kDa for VV IHD-J (Fig. 7). However, the CPV HA protein resembled the VV HA product in hemadsorption and fusion-inhibitor activities.

The $Fusion^+$ HAD^+ phenotype of SPI-3 mutants has been observed for the diverged orthopoxviruses raccoonpox virus and volepox virus (8b). Presumably wild-type raccoonpox virus is a natural SPI-3 mutant or synthesizes an HA which is HAD^+ but lacks fusion-inhibitor activity. The HAD and fusion-inhibitor activities of the VV HA can be separated by mutation to yield a rare $Fusion^-$ HAD^- variant (26), but $Fusion^+$ HAD^+ HA mutants have not been described previously.

The HA product could be altered in SPI-3 mutants such that it can no longer inhibit cell fusion. In wild-type virus, the SPI-3 product may inhibit processing of the HA protein by a host serine protease, thus preventing loss of fusion-inhibitor activity. It has been reported that treatment with trypsin increases the infectivity of VV by removing the fusion-inhibitor activity of the HA (20). Alternatively, the SPI-3 protein may have a direct role in fusion inhibition which is not mediated via HA. The localization of the SPI-3 protein in infected cells has not been determined. Unlike SPI-1 and SPI-2, the predicted SPI-3 product has a potential signal sequence near the amino terminus and a hydrophobic region near the carboxy terminus (28), suggesting that the SPI-3 protein may be secreted or membrane associated.

The similarity of cell fusion induced by SPI-3 mutants and HA mutants in terms of appearance under the microscope and sensitivity to MAbC3 suggests that the two genes are involved in a common fusion pathway which requires the 14-kDa protein. The observation that HA^- $SPI\text{-}3^-$ double

mutants were no more fusogenic than either single mutant (data not shown) is consistent with this idea. Other participants in the cell fusion process besides the 14-kDa protein are less clear. VV mutants lacking the 37-kDa protein of extracellular enveloped virus (EEV) are unable to fuse cells after the appropriate inducing treatment (3). This probably does not reflect a direct requirement for the 37-kDa protein but rather a requirement for the assembly of EEVs and their transport to the cell surface. Inhibition of low pH-induced fusion by rifampin (8a) is consistent with this notion. Production of EEV by SPI-3 mutants was normal (data not shown), suggesting that fusion was not triggered here by failure of a fusion inhibitor to reach the cell surface during virion release. Binding of HA to the 37-kDa protein has been reported (20). Experiments are in progress to generate antibodies to the SPI-3 protein to determine its location in infected cells and to look for interactions between the SPI-3 product and other proteins involved in cell fusion.

ACKNOWLEDGMENTS

We thank D. C. Bloom for supplying the cloned RPV *Hin*dIII K fragment, pHGN4.1, and RPV HA$^+$; S. Dales for anti-HA antiserum; and M. Esteban for MAbC3.

This work was supported by NIH grant AI-15722.

REFERENCES

1. **Archard, L. C., M. Mackett, D. E. Barnes, and K. R. Dumbell.** 1984. The genome structure of cowpox virus white pock variants. J. Gen. Virol. **65**:875–886.
2. **Beattie, E., J. Tartaglia, and E. Paoletti.** 1991. Vaccinia virus-encoded eIF-2α homolog abrogates the antiviral effect of interferon. Virology **183**:419–422.
3. **Blasco, R., and B. Moss.** 1991. Extracellular vaccinia virus formation and cell-to-cell virus transmission are prevented by deletion of the gene encoding the 37,000-dalton outer envelope protein. J. Virol. **65**:5910–5920.

3a. **Bloom, D. C.** Unpublished data.

4. **Bloom, D. C., K. M. Edwards, C. Hager, and R. W. Moyer.** 1991. Identification and characterization of two nonessential regions of the rabbitpox virus genome involved in virulence. J. Virol. **65**:1530–1542.
5. **Boursnell, M. E. G., I. J. Foulds, J. I. Campbell, and M. M. Binns.** 1988. Non-essential genes in the vaccinia virus HindIII K fragment: a gene related to serine protease inhibitors and a gene related to the 37K vaccinia virus major envelope antigen. J. Gen. Virol. **69**:2995–3003.
6. **Boyle, D. B., and B. E. H. Coupar.** 1988. A dominant selectable marker for the construction of recombinant poxviruses. Gene **65**:123–128.
7. **Brown, C. K., D. C. Bloom, and R. W. Moyer.** 1991. The nature of naturally occurring mutations in the hemagglutinin gene of vaccinia virus and the sequence of immediately adjacent genes. Virus Genes **5**:235–242.
8. **Brown, C. K., P. C. Turner, and R. W. Moyer.** 1991. Molecular characterization of the vaccinia virus hemagglutinin gene. J. Virol. **65**:3598–3606.

8a. **Doms, R. W.** Personal communication.

8b. **Esposito, J.** Personal communication.

9. **Esposito, J. J., and J. C. Knight.** 1985. Orthopoxvirus DNA: a comparison of restriction profiles and maps. Virology **143**:230–251.
10. **Esposito, J. J., J. F. Obijeski, and J. H. Nakano.** 1978. Orthopoxvirus DNA: strain differentiation by electrophoresis of restriction endonuclease fragmented virion DNA. Virology **89**: 53–66.
11. **Falkner, F. G., and B. Moss.** 1988. *Escherichia coli gpt* gene provides dominant selection for vaccinia virus open reading frame expression vectors. J. Virol. **62**:1849–1854.
12. **Goebel, S. J., G. P. Johnson, M. E. Perkus, S. W. Davis, J. P. Winslow, and E. Paoletti.** 1990. The complete DNA sequence of vaccinia virus. Virology **179**:247–266.
13. **Gong, S. C., C. F. Lai, and M. Esteban.** 1990. Vaccinia virus induces cell fusion at acid pH and this activity is mediated by the N-terminus of the 14-kDa virus envelope protein. Virology **178**:81–91.
14. **Higuchi, R.** 1990. PCR protocols: a guide to methods and applications, p. 177–183. Academic Press, Inc., New York.
15. **Hirt, P., G. Hiller, and R. Wittek.** 1986. Localization and fine structure of a vaccinia virus gene encoding an envelope antigen. J. Virol. **58**:757–764.
16. **Ichihashi, Y., and S. Dales.** 1971. Biogenesis of poxviruses: interrelationship between hemagglutinin production and polykaryocytosis. Virology **46**:533–543.
17. **Kotwal, G. J., and B. Moss.** 1989. Vaccinia virus encodes two proteins that are structurally related to members of the plasma serine protease inhibitor superfamily. J. Virol. **63**:600–606.
18. **Mackett, M., and L. C. Archard.** 1979. Conservation and variation in Orthopoxvirus genome structure. J. Gen. Virol. **45**:683–701.
19. **Moss, B.** 1990. Poxviridae and their replication, p. 2079–2112. *In* B. N. Fields and D. E. Knipe (ed.), Virology. Raven Press, New York.
20. **Oie, M., H. Shida, and Y. Ichihashi.** 1990. The function of the vaccinia hemagglutinin in the proteolytic activation of infectivity. Virology **176**:494–504.
21. **Palumbo, G. J., D. J. Pickup, T. N. Fredrickson, L. J. McIntyre, and R. M. L. Buller.** 1989. Inhibition of an inflammatory response is mediated by a 38-kDa protein of cowpox virus. Virology **172**:262–273.
22. **Pickup, D. J., B. S. Ink, W. Hu, C. A. Ray, and W. K. Joklik.** 1986. Hemorrhage in lesions caused by cowpox virus is induced by a viral protein that is related to plasma protein inhibitors of serine proteases. Proc. Natl. Acad. Sci. USA **83**:7698–7702.
23. **Pickup, D. J., B. S. Ink, B. L. Parsons, W. Hu, and W. K. Joklik.** 1984. Spontaneous deletions and duplications of sequences in the genome of cowpox virus. Proc. Natl. Acad. Sci. USA **81**:6817–6821.
24. **Rodriguez, J. F., R. Janeczko, and M. Esteban.** 1985. Isolation and characterization of neutralizing monoclonal antibodies to vaccinia virus. J. Virol. **56**:482–488.
25. **Rodriguez, J. F., E. Paez, and M. Esteban.** 1987. A 14,000-M_r envelope protein of vaccinia virus is involved in cell fusion and forms covalently linked trimers. J. Virol. **61**:395–404.
26. **Seki, M., M. Oie, Y. Ichihashi, and H. Shida.** 1990. Hemadsorption and fusion inhibition activities of hemagglutinin analyzed by vaccinia virus mutants. Virology **175**:372–384.
27. **Shida, H., and S. Dales.** 1982. Biogenesis of vaccinia: molecular basis for the hemagglutination-negative phenotype of the IHD-W strain. Virology **117**:219–237.
28. **Smith, G. L., S. T. Howard, and Y. S. Chan.** 1989. Vaccinia virus encodes a family of genes with homology to serine proteinase inhibitors. J. Gen. Virol. **70**:2333–2343.
29. **Tomley, F., M. Binns, J. Campbell, and M. Boursnell.** 1988. Sequence analysis of an 11.2 kilobase, near-terminal, BamHI fragment of fowlpox virus. J. Gen. Virol. **69**:1025–1040.

29a. **Turner, P. C., and R. W. Moyer.** Unpublished data.

30. **Upton, C., J. L. Macen, D. S. Wishart, and G. McFadden.** 1990. Myxoma virus and malignant rabbit fibroma virus encode a serpin-like protein important for virus virulence. Virology **179**: 618–631.